Chinese Chemical Letters 36 (2025) 110282

Contents lists available at ScienceDirect

Chinese Chemical Letters

journal homepage: www.elsevier.com/locate/cclet

Near-infrared light responsive upconversion-DNA nanocapsules for remote-controlled CRISPR-Cas9 genome editing

Yuqing Liu[a], Shiling Zhang[a], Kai Jiang[a], Shiyue Ding[a], Limei Xu[a], Yingqi Liu[a], Ting Wang[a], Fenfen Zheng[a,*], Weiwei Xiong[a,*], Jun-Jie Zhu[b,*]

[a] School of Environmental & Chemical Engineering, Jiangsu University of Science and Technology, Zhenjiang 212003, China
[b] State Key Laboratory of Analytical for Life Science, School of Chemistry and Chemical Engineering, Nanjing University, Nanjing 210023, China

ARTICLE INFO

Article history:
Received 4 February 2024
Revised 19 June 2024
Accepted 17 July 2024
Available online 18 July 2024

Keywords:
UCNPs
CRISPR/Cas9
Gene editing
DNA nanocapsules
Near-infrared light

ABSTRACT

As a renovator in the field of gene editing, CRISPR-Cas9 has demonstrated immense potential for advancing next-generation gene therapy owing to its simplicity and precision. However, this potential faces significant challenges primarily stemming from the difficulty in efficiently delivering large-sized genome editing system (including Cas9 protein and sgRNA) into targeted cells and spatiotemporally controlling their activity *in vitro* and *in vivo*. Therefore, the development of CRISPR/Cas9 nanovectors that integrate high loading capacity, efficient encapsulation and spatiotemporally-controlled release is highly desirable. Herein, we have engineered a near-infrared (NIR) light-activated upconversion-DNA nanocapsule for the remote control of CRISPR-Cas9 genome editing. The light-responsive upconversion-DNA nanocapsules consist of macroporous silica ($mSiO_2$) coated upconversion nanoparticles (UCNPs) and photocleavable *o*-nitrobenzyl-phosphate-modified DNA shells. The UCNPs act as a "nanotransducers" to convert NIR light (980 nm) into local ultraviolet light, thereby facilitating the cleavage of photosensitive DNA nanocapsules and enabling on-demand release of CRISPR-Cas9 encapsuled in the macroporous silica. Furthermore, by formulating a sgRNA targeted to a tumor gene (polo-like kinase-1, PLK-1), the CRISPR-Cas9 loaded UCNP-DNA nanocapsules (crUCNP-DNA nanocapsules) have effectively suppressed the proliferation of tumor cells through NIR light-activated gene editing both *in vitro* and *in vivo*. Overall, this UCNP-DNA nanocapsule holds tremendous potential for CRISPR-Cas9 delivery and remote-controlled gene editing in deep tissues, as well as the treatment of diverse diseases.

The clustered regularly interspaced short palindromic repeats (CRISPR)-associated protein 9 (Cas9) system stands out as one of the most promising tools in the arsenal of gene therapy [1,2]. It relies on engineered single guide RNAs (sgRNAs) for precise site recognition and corrects mutations through non-homologous end joining or homology-directed repair, offering a versatile platform poised to reform the treatment of diseases, including cancer [3]. Given the challenges associated with the simultaneous delivery of two macromolecules-cas9 (~160 kDa) and sgRNA (more than 100 base pairs), developing a safe and effective *in vivo* delivery system for CRISPR-Cas9 therapeutic components remains an urgent imperative [4,5]. The optimal advanced delivery system should simultaneously fulfill the requirements of high-dose cargo loading, efficient encapsulation, and controlled release functions.

Over the decades, the concept of on-demand gene delivery, relying on stimuli-responsive nanomaterial design, has been extensively explored in the field of nanomedicine [6-12]. These innovative strategies involve the incorporation of chemical moieties into nanocarriers, facilitating the triggered release of CRISPR/Cas9 genome editing machinery in response to specific endogenous environments (*e.g.*, low pH [13], redox-active species [14], and other disease-associated biomarkers [15]) or external stimuli (*e.g.*, light irradiation [16], magnetic fields [17], and ultrasound [18]). Among the diverse control strategies, photo-responsive genome editing delivery, regulated by light irradiation, offers a method for remote control of CRISPR/Cas9 release with high spatiotemporal resolution [19-21]. Since most photo-responsive molecules, such as azobenzene derivatives [22], spiropyran derivatives [23], and *o*-nitrobenzyl containing molecules [24], typically respond to high-energy ultraviolet (UV) light with limited penetration depth and carcinogenic risk [25,26], lanthanide-doped upconversion nanoparticles (UCNPs) have been developed to convert low-energy near-infrared radiation (800 or 980 nm) into high-energy ultraviolet

* Corresponding authors.
E-mail addresses: zhengfenfen@just.edu.cn (F. Zheng), xiongweiwei@just.edu.cn (W. Xiong), jjzhu@nju.edu.cn (J.-J. Zhu).

https://doi.org/10.1016/j.cclet.2024.110282
1001-8417/

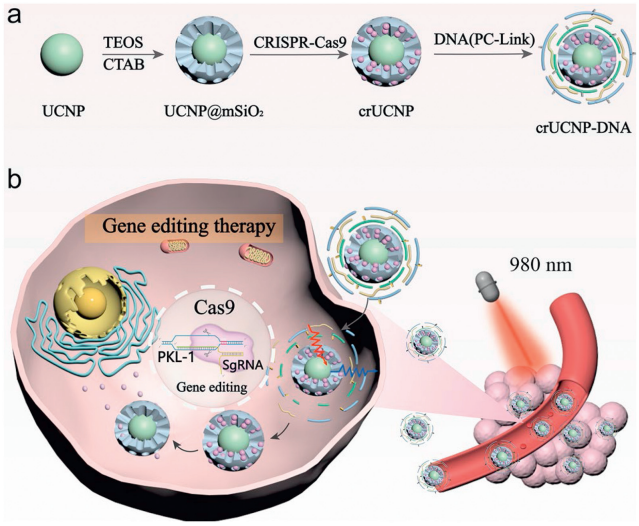

Fig. 1. Design NIR light–responsive UCNP-DNA nanocapsule for remote-controlled CRISPR-Cas9 gene editing. (a) Preparation of crUCNP-DNA nanocapsules. (b) NIR-triggered release of CRISPR-Cas9 to the cell nucleus for gene editing.

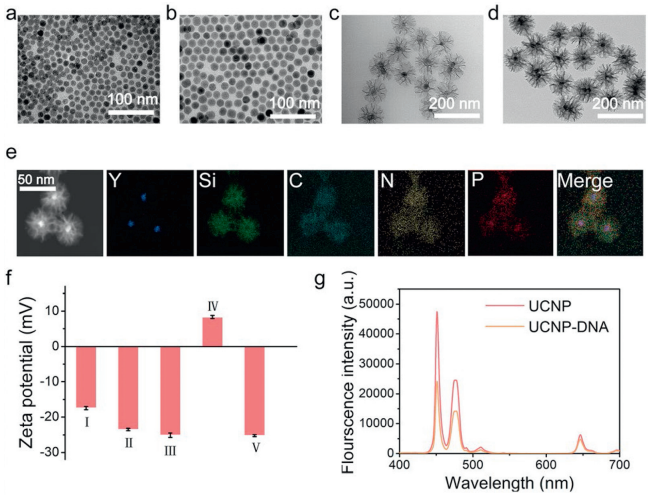

Fig. 2. Characterization of the nanocapsules. Transmission electron microscopy (TEM) images illustrating the morphology of (a) $NaYF_4$:Yb,Tm, (b) $NaYF_4$:Yb,Tm@$NaYF_4$, with scale bars of 100 nm. Additionally, TEM images representing (c) UCNP@$mSiO_2$, and (d) UCNP-DNA nanocapsules, with scale bars of 200 nm. (e) Energy-dispersive X-ray (EDX) elemental mapping of UCNP-DNA nanocapsules, with a scale bar of 50 nm. (f) Zeta potentials of (I) UCNP@$mSiO_2$, (II) CRISPR-Cas9, (III) UCNP@$mSiO_2$/CRISPR-Cas9, (IV) UCNP@$mSiO_2$/CRISPR-Cas9@PAH, and (V) crUCNP-DNA nanocapsules, arranged from left to right. (g) Fluorescence spectrum depicting the emission of UCNP and UCNP-DNA nanocapsules activated by a 980 nm laser.

or visible light, providing an appealing strategy for the remote manipulation of biomolecules and biological processes [27-31]. For instance, Pan *et al.* designed an upconversion nanoparticle (UCNP) capable of converting NIR to high energy UV light to control the release of Cas9 ribonucleoprotein (RNP) anchored on UCNP surface [32]. Similarly, Wu *et al.* developed a near-infrared (NIR) light-responsive CRISPR/Cas9 plasmid delivery system *via* a charge-nanovector, based on an ultraviolet-sensitive conjugated polyelectrolyte covered on an upconversion nanomaterial [33]. Although valuable, grafting large-sized CRISPR/Cas9 onto the surface of the nanoparticles not only limits their loading capacity but also makes them prone to degradation during circulation. Therefore, there is an urgent need to develop CRISPR/Cas9 nanovectors that combine high loading capacity, efficient encapsulation, and spatiotemporally-controlled release.

Herein, we devised a near-infrared (NIR) light-responsive nanovector for spatiotemporally controlled release of Cas9/sgRNA in cancer therapy based on UCNP-DNA nanocapsules. As illustrated in Fig. 1, the nanovector comprises three key components: (1) upconversion luminescent nanoparticles $NaYF_4$:Yb,Tm@$NaYF_4$ capable of emitting intense UV light upon 980 nm laser irradiation; (2) dendrimeric macroporous silica shell with a substantial pore volume designed for loading Cas9/sgRNA targeting the cancer therapeutic gene polo-like kinase 1 (PLK-1); (3) DNA nanocapsules, comprised of UV-responsive cleavable DNA with an *o*-nitrobenzyl-phosphate motif, are employed for encapsulating Cas9/sgRNA and enabling spatiotemporally controlled gene editing through UCNP-mediated photo-conversion.

To obtain upconversion nanoparticles emitting blue light, $NaYF_4$:Yb,Tm@$NaYF_4$ core-shell UCNPs were synthesized *via* a previously reported thermal decomposition method [34]. Transmission electron microscopy (TEM) images reveal highly homogeneous UCNPs, along with an average size increasing from 17 nm to 21 nm after coating with $NaYF_4$ shell (Figs. 2a and b). X-ray diffraction (XRD) spectra confirm that peak positions and intensities of the as-prepared UCNPs align with those of the pure hexagonal-phase $NaYF_4$:Yb,Tm@$NaYF_4$ nanocrystals (JCPDS No. 28–1192, Fig. S1 in Supporting information). To enhance the nanoparticles' loading capacity for macromolecules, dendritic macroporous silica shells were coated on the surface of UCNPs through an oil-water two-phase reaction system [35]. The resulting UCNP@$mSiO_2$ nanoparticles showed an increased diameter of 110 nm with a large pore size of 20–30 nm, facilitating the loading of Cas9/sgRNA (Fig. 2c). The sgRNA, targeting the PLK-1 gene associated with various cancer types [36], was synthesized by using an RNA kit. The as-prepared sgRNA was characterized by denaturing Gel electrophoresis confirmed the high purity of the synthesized sgRNA (Fig. S2 in Supporting information). Subsequently, the editing ability of Cas9/sgRNA on the target gene PLK-1 was explored. Compared to untreated PLK-1 DNA or sgRNA-treated PLK-1 DNA, several lower molecular-wight bands appeared in Cas9/sgRNA-treated PLK-1 DNA (lane III) (Fig. S3 in Supporting information). The result indicates that the Cas9/sgRNA could knocked out the target gene PLK-1 and thus inhibit cell proliferation and induce apoptosis by deletion of the protein encoded by this gene. Then, Cas9/sgRNA was loaded into the pore of UCNP@$mSiO_2$. To quantify the loaded or released Cas9/sgRNA, Cas9 protein was labeled with ICG for visualization. The amount of Cas9/sgRNA loaded into UCNP@$mSiO_2$ was determined to be 566.5 mg/g (Fig. S8 in Supporting information). As expected, the specific surface area and pore volume were decreased from 231.51 m^2/g and 16.109 nm to 62.898 m^2/g and 11.598 nm, respectively, due to the encapsulation of Cas9/sgRNA in the pore structures (Figs. S4 and S5 in Supporting information).

Moreover, to achieve remote NIR-controlled gene editing, DNA strands containing *o*-nitrobenzyl phosphate photoreactive molecule that can be cleaved by ultraviolet light were deposited on the surface of cationic polymer polyacrylamide hydrochloride (PAH) modified UCNP@$mSiO_2$ nanoparticles through layer-by-layer self-assembly, thereby forming light-responsive UCNP-DNA nanocapsules. The DNA nanocapsule coating could be identified in the TEM by the increased contrast (Fig. 2d). Elemental mapping of the UCNP-DNA nanocapsules further validated the core/shell/shell geometry and composition, incorporating Y in the UCNP core, Si in the $mSiO_2$ shell, and N, C, P in the DNA nanocapsule (Fig. 2e). The gradual increase in hydrodynamic diameter and reversed zeta potential once again affirmed the successful assembly of the UCNP-DNA nanocapsules (Fig. 2f and Fig. S6 in Supporting information). Notedly, both UCNPs and UCNP-DNA nanocapsules exhibit multiple luminescent properties, characterized by robust blue emis-

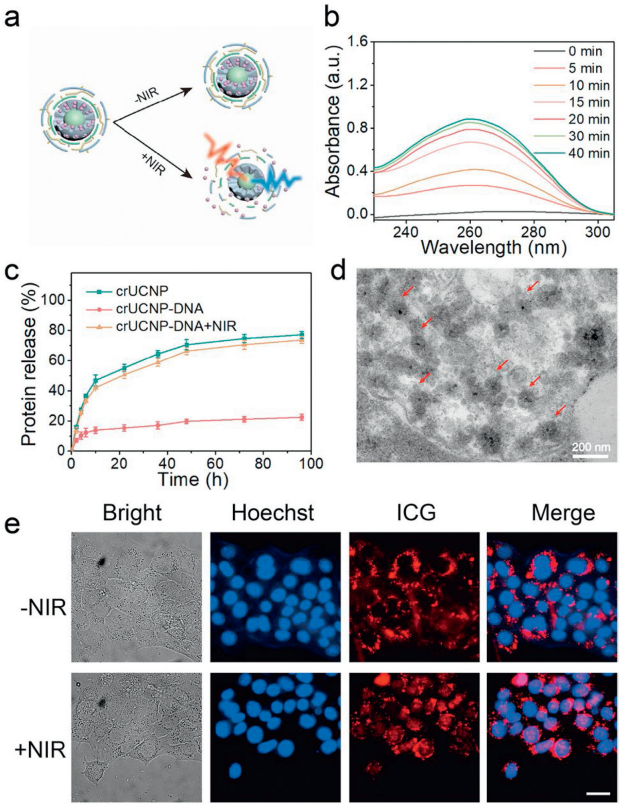

Fig. 3. Near-infrared photorelease protein validation. (a) Illustration depicting the schematic of protein release from crUCNP-DNA nanocapsules triggered by near-infrared light. (b) Ultraviolet absorption of crUCNP-DNA supernatant at different time irradiated by 980 nm laser. (c) Protein release at pH 5.5. (d) Bio-TEM images of 4T1 cells post-incubation with crUCNP-DNA nanocapsules for 24 h. (e) Fluorescence microscope image of crUCNP-DNA nanocapsules treated cells for 24 h with or without irradiation. Scale bar: 20 μm. Red: Cas9 labeled with ICG; Blue: nuclei stained with Hoechst 33342.

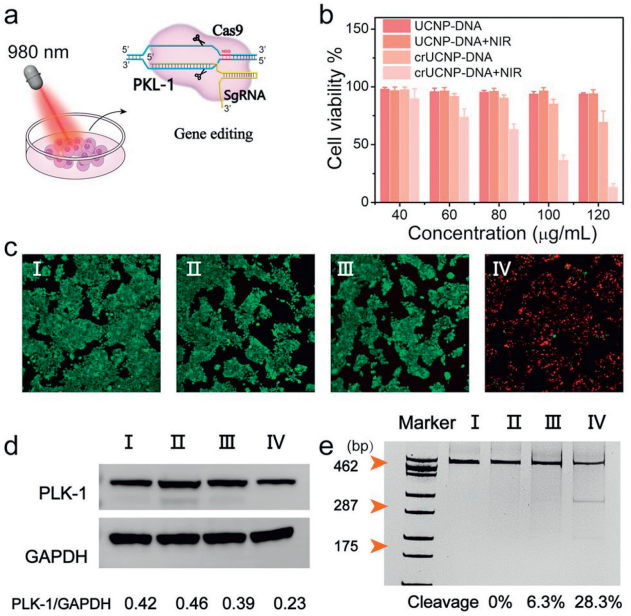

Fig. 4. (a) Schematic diagram of intracellular gene editing activated by near-infrared light. (b) MTT analysis of 4T1 cells subjected to different treatments. (c) Fluorescence images of 4T1 cells co-stained with calcein AM/PI post-treatment with various formulations. Scale bar: 100 μm (Green: calcein-AM; Red: PI). (d) Western blot assay. (e) T7EI assay. (I) Pure media + NIR, (II) UCNP-DNA nanocapsules + NIR, (III) crUCNP-DNA nanocapsules, and (IV) crUCNP-DNA nanocapsules + NIR.

sion, suitable for activating UV-sensitive groups on DNA nanocapsules (Fig. 2g). To prove the NIR-responsive activation of UCNP-DNA nanocapsules (Fig. 3a), ultraviolet-visible analysis was performed on UCNP-DNA nanocapsules supernatant after 980 nm laser irradiation (Fig. 3b). The absorbance change of DNA at 260 nm demonstrated that UCNPs embedded in UCNP-DNA nanocapsules could convert NIR light (980 nm) to local ultraviolet light for collapsing the photosensitive DNA nanocapsules. This process may ultimately result in the on-demand release of CRISPR-Cas9 encapsulated in macroporous silica.

To further explore the NIR responsive release of CRISPR-Cas9 from the CRISPR-Cas9 loaded UCNP-DNA nanocapsules (crUCNP-DNA nanocapsules), we labeled Cas9 in crUCNP-DNA nanocapsules with ICG (Fig. S7 in Supporting information). The release profile of CRISPR-Cas9 from the nanocapsules was recorded at 790 nm using a UV–vis spectrophotometer. As depicted in Fig. S9 (Supporting information), the UCNP@mSiO_2 without DNA nanocapsule encapsulating exhibited a low release rate under normal physiological environment (pH 7.4), while sustained release was observed at pH 5.5. After encapsulating with the DNA nanocapsules, the release rate of Cas9 at pH 5.5 was less than 20%, attributed to the protective effect of the DNA nanocapsules. Upon irradiation with NIR light for 10 min, the UV light emitted from UCNP ruptured the photoresponsive DNA nanocapsules, leading to a high release rate of around 70%, a value comparable to that of the nanovectors without DNA encapsulation (Fig. 3c). This outcome underscores the capability of photoresponsive UCNP-DNA nanocapsules to achieve controlled release through NIR light exposure.

To assess the cellular uptake and subcellular distribution of the nanocapsules, Cas9 protein was labeled with ICG to enhance visibility. 4T1 cells were incubated with the crUCNP-DNA nanocapsules, and the near-infrared fluorescence signals of ICG were monitored at different time points using fluorescence microscopy. The fluorescence imaging results revealed that a majority of the nanocapsules were internalized by endosomes-/lysosomes within 4 h and subsequently escaped into the cytoplasm during extended incubation (Fig. S11 in Supporting information). The inductively coupled plasma optical emission spectrometer (ICP-OES) was used to detect the content of Y element in the cells treated with crUCNP-DNA nanocapsules at different time points. It was found that the uptake of crUCNP-DNA nanocapsules reached the maximum at 12 h (Fig. S11). Therefore, 980 nm light treatment was conducted on 4T1 cells after incubating with the nanocapsules for 12 h in follow-up experiments. TEM images further confirmed the presence of the nanocapsules in the cytoplasm after internalization into 4T1 cells for 24 h (Fig. 3d).

We further investigated the capability of the UCNP-DNA nanocapsules for releasing target molecule within 4T1 cells. As depicted in Fig. 3e, weak fluorescence of Cas9-ICG was mainly observed in lysosomes and cytoplasm of 4T1 cells without NIR light irradiating. Upon treatment with NIR light, fluorescence imaging revealed the entry of some Cas9-ICG molecules into the nucleus (Fig. 3e). This further underscores the competence of our engineered light-responsive UCNP-DNA nanocapsules for achieving light-controlled release of CRISPR-Cas9 system within cells.

Prior to assessing its genome editing capability in cells (Fig. 4a), we conducted evaluations on the biocompatibility of UCNP-DNA nanocapsules and the biosafety of NIR laser exposure. 4T1 cells were exposed to different doses of UCNP-DNA nanocapsules, and cell viability was determined by MTT assay after 72 h. As shown in Fig. 4b, the UCNP-DNA nanocapsules at concentrations below 100 μg/mL exhibited no adverse effects on cell viability. Subsequently, 4T1 cells incubated with UCNP-DNA nanocapsules (100 μg/mL) for 12 h were irradiated with 980 nm laser at different

power levels to assess the toxicity of UCNP-DNA excited UV light. The results indicated that there was no significant attenuation in the viability of the treated 4T1 cells under the given conditions (Fig. S12 in Supporting information), which could be attributed to the located nature of UCNP-generated UV light, with *o*-nitrobenzyl phosphate in the DNA nanocapsules absorbing a portion of the converted UV light. Recognizing the potential temperature increase due to water absorbing 980 nm laser light, we addressed this concern by employing short irradiation periods (30 s of irradiation followed by a 30 s interruption) in our experiments.

Building upon the evidence of the remarkable biocompatibility of nanocapsules and efficient release of CRISPR-Cas9 from light-responsive UCNP-DNA nanocapsules, our subsequent investigation delved into inhibiting tumor proliferation through NIR-responsive genome editing in 4T1 cells with high expression of PLK-1 gene [37]. 4T1 cells were incubated with crUCNP-DNA nanocapsules for 12 h and then exposed to 980 nm NIR light for 20 min before further incubation (irradiation for 30 s followed by a 30 s break). At 72 h, cell viability was assessed by MTT assay. As shown in Fig. 4b, the viability of the cells treated with the crUCNP-DNA nanocapsules plus NIR irradiation exhibited a significant decrease compared to other groups. This suggests that NIR irradiation effectively triggered photocleavage reactions of DNA nanocapsules, leading to the release of CRISPR-Cas9 for gene editing. Fluorescence images further corroborated these findings, revealing the weakest green intensity for calcein AM (stained live cells) and the highest red intensity for propidium iodide (PI) (stained dead cells) in the cells incubated with crUCNP-DNA nanocapsules plus NIR irradiation (Fig. 4c). These results aligned with the MTT assay outcomes. Additionally, flow cytometry analysis produced similar results (Fig. S13 in Supporting information).

To ascertain whether apoptosis primarily resulted from the inhibition of PLK-1 protein expression, we lysed cells to extract proteins for Western blot analysis. As shown in Fig. 4d, the cells treated with crUCNP-DNA nanocapsules plus NIR irradiation exhibited lower PLK-1 protein expression compared controls. Subsequently, we quantified the mutation frequency using the SURVEYOR assay, revealing a high mutation frequency in the target gene of cells treated with crUCNP-DNA nanocapsules plus NIR irradiation (Fig. 4e). In contrast, 4T1 cells incubated with other groups exhibited ignorable mutation frequencies (Fig. 4e), further demonstrating the significance of NIR as an on/off switch for precisely controlled gene therapy.

Inspired by the successful NIR-controlled activation and outstanding therapeutic efficiency of the crUCNP-DNA nanocapsules *in vitro*, we proceeded to explore their behavior *in vivo*. Animal experiments were conducted in accordance with the guidelines of the Institutional Animal Care and Use Committee of Jiangsu University of Science and Technology. Initially, the biodistribution and metabolism of the UCNP-DNA nanocapsules were investigated in xenograft mice bearing 4T1 cells by fluorescence imaging. The *in vivo* imaging results illustrated prolonged accumulation of the crUCNP-DNA nanocapsules at the tumor site (Fig. 5a). *Ex-vivo* imaging of organs and tumors and fluorescence intensity quantification 96 h after injection revealed significant accumulation of nanocapsules in the liver and spleen (Fig. 5b and Fig. S14 in Supporting information), suggesting that the UCNP-DNA nanocapsules were presumably metabolized through the reticuloendothelial system [38].

Then, the *in vivo* therapeutic efficacy of the designed crUCNP-DNA nanocapsules was investigated by administrating the mice with different formulations *via* intravenous injection. After injection, the mice underwent NIR light irradiation for 20 min (2.0 W/cm^2, 30 s on and 30 s off) every other day. After a 20-day treatment period, the tumor sizes in PBS + NIR group and UCNP-DNA nanocapsules group with or without NIR light irradiation had

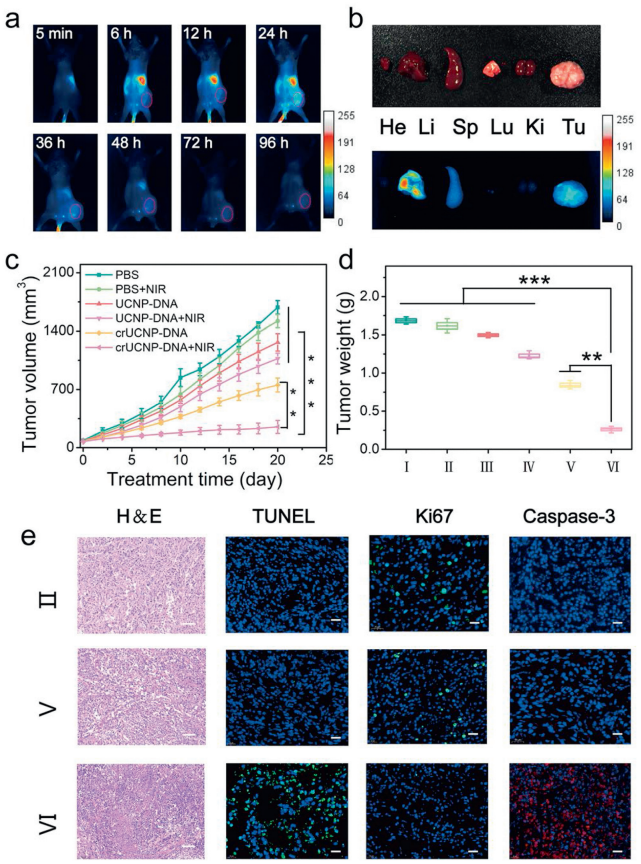

Fig. 5. (a) Fluorescence images taken at different intervals after tail vein injection of crUCNP-DNA nanocapsules in 4T1 hormonal mice. (b) Fluorescence images of isolated organs and tumors in mice. (He: Heart; Li: Live; Sp: Spleen; Lu: Lung; Ki: Kidney; Tu: Tumor). (c) Tumor sizes following diverse treatments as indicated. (d) Combined analysis of tumor weights from mice after different treatments (I-VI) (from left to right). (e) Histopathological assessment of mouse tumors (II, V, VI), including H&E staining (scale bar: 200 μm), TUNEL staining (scale bar: 20 μm), Ki67 antigen staining (scale bar: 20 μm), caspase-3 staining (scale bar: 20 μm). (I) PBS, (II) PBS + NIR, (III) UCNP-DNA nanocapsules, (IV) UCNP-DNA nanocapsules + NIR, (V) crUCNP-DNA nanocapsules, and (VI) crUCNP-DNA nanocapsules + NIR. ($^*P < 0.05$, $^{**}P < 0.01$, $^{***}P < 0.001$ analyzed by Student's *t*-test.)

dramatically grown, signifying the negligible inhibition efficacy of these formulations (Fig. 5c). What is more, a notable contrast in tumor volume was observed between the crUCNP-DNA nanocapsules with and without NIR light irradiation, highlighting the significance of NIR light irradiation in remote-controlled CRISPR-Cas9 genome editing for inhibiting tumor growth. In addition, the anticancer efficacy was evaluated through weighing and photographing the tumors collected from the sacrificed mice (Fig. 5d and Fig. S15a in Supporting information). The inhibition ratio of the crUCNP-DNA nanocapsules with NIR light irradiation was calculated to be 84.1%, exhibiting more prominent anticancer efficacy than the crUCNP-DNA nanocapsules without NIR light irradiation 45.1%. The superior anticancer potency of the crUCNP-DNA nanocapsules was attributed to the high encapsulation rate of the DNA nanocapsules and the effective release of CRISPR-Cas9 facilitated by NIR light irradiation. Meanwhile, no significant weight loss was observed during the treatment period (Fig. S15b in Supporting information), suggesting insignificant side effect of these treatments on the mice. Subsequently, hematoxylin and eosin (H&E) staining and terminal deoxynucleotidyl transferase dUTP nick end labeling (TUNEL) in tumor tissues were performed to reveal the therapeutic efficacy of the crUCNP-DNA nanocapsules. H&E staining showed a decrease in cell density after administration of crUCNP-DNA nanocap-

sules + NIR (Fig. 5e). *In situ* TUNEL assay displayed a significant enhancement of bulk apoptosis in crUCNP-DNA nanocapsules treated tumors after NIR light irradiation (Fig. 5e). In contrast, the other groups showed minimal inhibition of tumor growth. Furthermore, caspase-3 tagging for apoptosis and Ki67 antigen labeling for cell proliferation also exhibited substantial differences after NIR radiation (Fig. 5e), verifying the controlled therapeutic effect of NIR light irradiation. Moreover, histological analyses of major organs in different groups of mice revealed no obvious abnormalities or significant organ damage (Fig. S16 in Supporting information). Collectively, the developed NIR light-responsive UCNP-DNA nanocapsules can effectively deliver and release the CRISPR-Cas system for gene therapy with high efficacy and low side effects.

In summary, we have developed UCNP-DNA nanocapsules for the delivery of CRISPR-Cas9 and the remote control of gene editing in cancer therapy by NIR light irradiation. In this innovative nanocapsule, UCNPs are set as a "nanotransducers" to translate NIR light (980 nm) into local ultraviolet light, macroporous silica acts as the container for CRISPR-Cas9, and the outermost DNA nanocapsules serves as a protecting shell responsive to the ultraviolet light emitted by UCNPs. Once internalized by cancer cells, UCNPs emit UV light to initiate the disintegration of the photoresponsive DNA nanocapsules under NIR light irradiation, thereby leading to the release of Cas9/sgRNA and the activation of gene editing. The crUCNP-DNA nanocapsules have demonstrated significant efficacy in inhibiting tumor cell proliferation and tumor growth through NIR light-activated gene editing. Overall, this UCNP-DNA nanocapsule combines the advantages of high cargo loading, efficient encapsulation, and remotely-triggered release, making it a promising cadidate for CRISPR-Cas9 delivery and spatiotemporally-controlled gene editing in cancer therapy.

Declaration of completing interest

The authors declare that they have no known competing financial interests or personal relationships that could have appeared to influence the work reported in this paper.

CRediT authorship contribution statement

Yuqing Liu: Writing – original draft, Methodology, Investigation, Data curation. **Shiling Zhang:** Investigation, Data curation. **Kai Jiang:** Methodology, Investigation, Data curation. **Shiyue Ding:** Validation, Software. **Limei Xu:** Visualization, Methodology. **Yingqi Liu:** Investigation, Data curation. **Ting Wang:** Validation, Methodology. **Fenfen Zheng:** Writing – review & editing, Supervision, Conceptualization. **Weiwei Xiong:** Supervision, Funding acquisition. **Jun-Jie Zhu:** Writing – review & editing, Supervision.

Acknowledgments

This work was financially supported by the National Natural Science Foundation of China (Nos. 21804059 and 21701059), the Natural Science Foundation of Jiangsu Province (No. BK20180974), the China Postdoctoral Science Foundation (No. 2020M681544), and the Postdoctoral Science Foundation of Jiangsu Province (No. 2020Z351).

Supplementary materials

Supplementary material associated with this article can be found, in the online version, at doi:10.1016/j.cclet.2024.110282.

References

[1] H.X. Wang, M. Li, C.M. Lee, et al., Chem. Rev. 117 (2017) 9874–9906.
[2] S.W. Cho, S. Kim, J.M. Kim, et al., Nat. Biotechnol. 31 (2013) 230–232.
[3] F. Jiang, J.A. Doudna, Annu. Rev. Biophys. 46 (2017) 505–529.
[4] K. Huang, D. Zapata, Y. Tang, et al., Biomaterials 291 (2022) 121876.
[5] Y.Q. Lin, K.K. Feng, J.Y. Lu, et al., J. Control. Release 361 (2023) 727–749.
[6] C. Zhuo, J. Zhang, J.H. Lee, et al., Signal Transduct. Target. Ther. 6 (2021) 238.
[7] P. Ma, Q. Wang, X. Luo, et al., Biomater. Sci. 11 (2023) 5078–5094.
[8] L. Li, Z. Yang, S. Zhu, et al., Adv. Mater. 31 (2019) e1901187.
[9] F. Zheng, W. Xiong, S. Sun, et al., Nanophotonics 8 (2019) 391–413.
[10] J. Sun, K. Jiang, Y. Wang, et al., Adv. Healthc. Mater. 12 (2023) 2302016.
[11] D. Jiang, Y. Pan, H. Yao, et al., Anal. Chem. 94 (2022) 9074–9080.
[12] H. Yao, D. Jiang, G. Dong, et al., Analyst 146 (2021) 5115–5123.
[13] R. Xie, X. Wang, Y. Wang, et al., Adv. Mater. 34 (2022) e2110618.
[14] E. Tan, T. Wan, C. Yu, et al., Nano Today 46 (2022) 101617.
[15] C. Zhang, X. Wang, G. Liu, et al., Small 19 (2023) e2206981.
[16] Y.A. Aksoy, B. Yang, W. Chen, et al., ACS Appl. Mater. Interfaces 12 (2020) 52433–52444.
[17] C. Zhuo, H. Kong, K. Yi, et al., Adv. Funct. Mater. 33 (2023) 2210860.
[18] H. Yin, L. Sun, Y. Pu, et al., ACS Cent. Sci. 7 (2021) 2049–2062.
[19] H. Yu, M.T. Kifle, L. Chen, et al., Sci. China Chem. 67 (2023) 664–676.
[20] H. Zhao, W. Hu, H. Ma, et al., Adv. Funct. Mater. 27 (2017) 1702592.
[21] D. Wang, L. Chen, C. Li, et al., J. Nanobiotechnol. 20 (2022) 27.
[22] H.M. Bandara, S.C. Burdette, Chem. Soc. Rev. 41 (2012) 1809–1825.
[23] R. Klajn, Chem. Soc. Rev. 43 (2014) 148–184.
[24] T. Liu, B. Bao, Y. Li, et al., Prog. Mater. Sci. 146 (2023) 101741.
[25] K. Jiang, Z. Guan, Y. Wang, et al., Anal. Chem. 95 (2023) 17392–17399.
[26] J. Wang, H. Qiu, Y. Xu, et al., Bioact. Mater. 11 (2022) 154–165.
[27] Y. Zhang, L. Huang, Z. Li, et al., ACS Nano 10 (2016) 3881–3885.
[28] R. Yan, Y. Guo, X. Wang, et al., ACS Nano 16 (2022) 8399–8418.
[29] F. Zheng, C. Wang, T. Meng, et al., ACS Nano 13 (2019) 12577–12590.
[30] T. Wang, K. Jiang, Y. Wang, et al., Chem. Sci. 15 (2024) 1829–1839.
[31] S. Zhi, X. Zhang, J. Zhang, et al., ACS Nano 17 (2023) 13533–13544.
[32] Y.C. Pan, J.J. Yang, X.W. Luan, et al., Sci. Adv. 5 (2019) eaav7199.
[33] Y. Wu, J. Zheng, Q. Zeng, et al., Nano Res. 13 (2020) 2399–2406.
[34] J. Yuan, Y. Cen, X.-J. Kong, et al., ACS Appl. Mater. Interfaces 7 (2015) 10548–10555.
[35] S. Liu, W. Li, S. Dong, et al., Nanoscale 12 (2020) 24146–24161.
[36] J. Dong, N. Nguyen, R. Ezhilarasan, et al., Neuro-Oncology 17 (2015) 18–40.
[37] B. Schrörs, S. Boegel, C. Albrecht, et al., Front. Oncol. 10 (2020) 1195.
[38] S. Sindhwani, A.M. Syed, J. Ngai, et al., Nat. Mater. 19 (2020) 566–575.